

THE IMPRINT OF PRESUPERNOVA WINDS ON SUPERNOVA REMNANT EVOLUTION: TOWARDS MORE REALISTIC MODELS FOR TYPE IA SUPERNOVA REMNANTS AND THEIR SPECTRA

C. Badenes and E. Bravo

¹Dpt. Physics and Nuclear Engineering, Univ.Polit.Catalunya, Diagonal 647, 08028 Barcelona, Spain

²Institute for Space Studies of Catalonia, Gran Capità 2-4, 08034 Barcelona, Spain

ABSTRACT

Supernova remnants are usually analysed in the light of hydrodynamical models of the interaction of supernova ejecta with either a constant density ambient medium or a circumstellar medium produced by a constant presupernova wind. However, the ejection of energetic wind during the presupernova phase changes the ambient medium structure and, consequently, the early supernova remnant evolution. We have analysed the evolution of young remnants of type Ia supernovae, focusing on the imprint of the presupernova wind history on the supernova remnant structure and on the influence of the explosion mechanism. We have found that the remnant evolution is most sensitive to the explosion mechanism at ages not larger than a few hundred years, while the presupernova history shows its influence at later epochs, before the Sedov phase sets in.

Key words: circumstellar matter – stars: winds, outflows – supernova remnants – supernovae: general

1. INTRODUCTION

Supernovae have become one key piece in the knowledge building of modern astronomy. They stand at the cornerstone of many fields, including cosmology, galactic and stellar evolution, cosmic rays generation, and many others. Type Ia supernovae (SNIa) are currently used as practical tools to measure cosmological distances and obtain insight about what kind of Universe we are in. However, the theoretical knowledge of SNIa is still plagued by uncertainties about the nature of their progenitor systems and the nature of the explosion mechanism.

Modern X-ray observatories, like *Chandra* and *XMM-Newton* give the opportunity to collect a huge amount of high quality, high resolution, data about supernova remnants (SNRs). Whereas the atomic codes that allow to compute and fit the X-ray spectra have experienced a considerable improvement in the last years, this is not the case of our knowledge of the hydrodynamical evolution of SNRs. There are two desirable directions of advance for our theoretical understanding of SNR evolution: one is multi-dimensional hydrodynamical simulations, and the other is one-dimensional hydrodynamical calculations,

that allow more realistic and more detailed supernova (SN) models. Here, we have focused on the last kind of studies.

Presupernova evolution is often neglected in the hydrodynamic simulations of type Ia SNR, because the mass loss episodes of the progenitors are not believed to have a deep influence on their circumstellar medium (CSM). The shaping of the CSM through stellar winds and the formation of wind bubbles have been studied extensively for massive early type stars (i.e., type II SN progenitors), albeit only for constant mass loss episodes or combinations of them (Weaver et al. 1977, Chevalier & Liang 1989). Up to now, the usual assumptions for the CSM surrounding type Ia SN progenitors have been either a constant density interstellar medium (ISM) or a power law CSM merging smoothly with the ISM. However, recent models of type Ia presupernova evolution predict substantial non-constant mass loss episodes during the binary evolution (Hachisu, Kato & Nomoto 1996, Langer et al. 2000). Evidence for this kind of behavior has been found in X-rays even for type II events (Immler, Aschenbach & Wang 2001). Light echoes have been detected around two overluminous type Ia supernovae: SN 1991T (Schmidt et al. 1994) and SN 1998bu (Cappellaro et al. 2001), which have been attributed to the presence of circumstellar dust. Thus, it is now necessary to evaluate the influence of such non-constant presupernova winds on the properties of the SNR.

The explosion mechanism of SNIa is still a matter of strong debate. Since the evolution of young SNRs is dominated by the SN ejecta profile, different explosion mechanisms (implying different ejecta profiles) can lead to important variations in the remnant behavior at early stages. Dwarkadas & Chevalier (1998) found that most ejecta profiles could be adjusted by an exponential profile, but also that this approach fails to reproduce many features of SNR evolution. Their results call for a more thorough study of the influence of the explosion mechanism on the properties of SNRs.

2. MODELS AND RESULTS

We have followed with an hydrodynamical code the interaction of the presupernova wind with the surrounding ISM up to the time of SN explosion. The code was the same as in Badenes & Bravo (2001), modified to take into account the radiative losses, which are dynamically meaning-

Table 1. Characteristics of wind models.

Wind model	v_w (km s ⁻¹)	M_w (M_\odot)	K_{51} ($\times 10^{51}$ ergs)	t_{end} (Myr)	t_{SN} (Myr)	R_s ($\times 10^{19}$ cm)	$R_{s,\text{Weaver}}$ ($\times 10^{19}$ cm)
A	200	0.2	8×10^{-5}	0.2	0.7	3.2	2.6
B	20	0.2	8×10^{-7}	0.2	0.7	1.4	1.0
C	200	0.6	2.4×10^{-4}	1.5	1.5	5.0	4.5
D	20	0.6	2.4×10^{-6}	1.5	1.5	2.0	1.8

NOTE.- v_w is the wind velocity, M_w is the total mass ejected in the wind, and K_{51} is the total kinetic energy of the wind; t_{end} is the duration of the wind phase, and t_{SN} is the time of the SN explosion; R_s and $R_{s,\text{Weaver}}$ are the radius of the outer shell at the time of SN explosion, according to the present calculations and to Weaver et al. (1977), respectively.

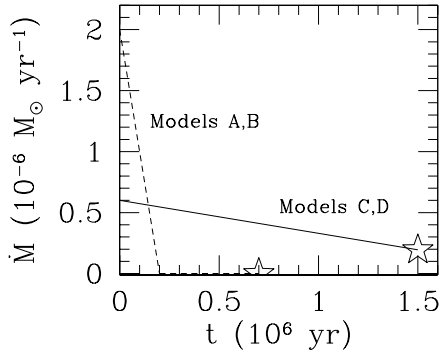


Figure 1. Time evolution of wind mass-loss rate for models A and B (dashed line) and models C and D (solid line). The time at which the SN explodes is identified by a star. Note that in models A and B the wind ends 0.5 Myr before SN explosion.

ful during the wind-ISM interaction. We have computed four cases corresponding to different wind models, whose characteristics can be found in Table 1 and Figure 1 (the ISM was always assumed to be initially homogeneous). Figure 2 displays the CSM profile for each model at the time of the SN explosion.

The results of the hydrodynamic computation of wind-ISM interaction have been used as the start configuration for the hydrodynamic calculation of SNR evolution. In this study of the influence of different wind models we have used an analytic ejecta profile given by an exponential law. The results are shown in Figures 3 and 4, together with the evolution of the same ejecta profile interacting with a constant density ISM. We use the shock expansion parameters ($\eta \equiv d \ln r / d \ln t$) of the forward and reverse shocks as a figure of merit for model comparison. It can be seen that the wind ejected by the progenitor system of a SNIa can have a dramatic influence on the dynamical

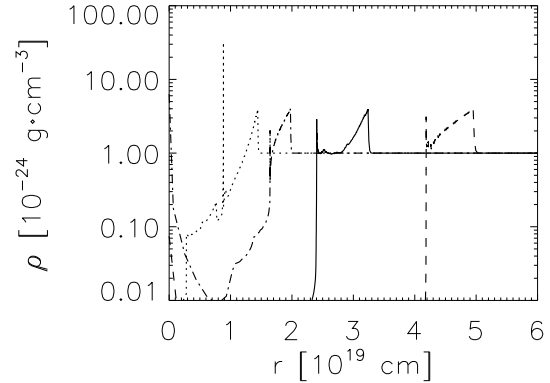


Figure 2. Circumstellar medium density profile for each wind model at the time of SN explosion. Lines correspond to wind models A (solid line), B (dotted line), C (dashed line), and D (dash-dotted line).

evolution of its SNR. This evolution cannot be accurately described with the usual assumptions of a power law CSM merging smoothly with the ISM or direct interaction between the ejecta and the ISM (see also Badenes & Bravo 2001).

We have also made a preliminary study of the influence of the explosion model on the SNR properties. We have chosen a few representative models of SNIa explosion (see Table 2): a delayed detonation (DDT), a pulsating delayed detonation (PDD), a deflagration (DEF) and a sub-Chandrasekhar explosion (SCH). In Figure 5, we compare them with the most usual analytical profiles: an exponential (EXP) and a power law with index 7 (PWL), both with ejected mass $1.4 M_\odot$ and kinetic energy 10^{51} erg.

The interaction of the different explosion models with a homogeneous ISM has been followed with the same hydrodynamical code. The evolution of the forward shock expansion parameter is given in Figures 6 and 7 (the evolution of the reverse shock expansion parameter shows only minor deviations between the different models and is not shown). It can be seen that the dynamical behavior of SNRs resulting from realistic SNIa explosion models

Table 2. Characteristics of the SNIa explosion models.

Explosion model	M_{ej} (M_{\odot})	K_{51} ($\times 10^{51}$ ergs)	t' (10^9 s)	M_{Fe} (M_{\odot})	M_{Ca} (M_{\odot})	M_{S} (M_{\odot})	M_{Si} (M_{\odot})	$M_{44\text{Ti}}$ (M_{\odot})
DEF	1.38	0.79	11.4	0.68	0.006	0.022	0.031	4.7×10^{-6}
DDT	1.37	2.00	7.1	1.04	0.023	0.069	0.084	5.6×10^{-5}
PDD	1.36	1.52	8.2	0.83	0.020	0.070	0.090	1.1×10^{-5}
SCH	0.97	0.98	7.7	0.49	0.027	0.102	0.141	1.2×10^{-3}

NOTE.- M_{ej} and K_{51} are, respectively, the ejected mass and the total kinetic energy released, and t' is the normalization timescale (see Figs. 6 and 7). The rest of columns give the yields of selected species. See Bravo et al. (1996) for more details on the models.

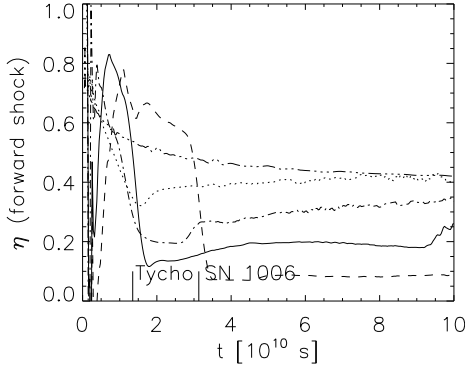


Figure 3. Expansion parameter of the forward shock as a function of time for the interaction of an exponential ejecta profile with the CSM as modified by the four wind models (see Fig.2), together with the interaction of the exponential ejecta with a constant density ISM (triple-dot-dashed line). The ages of Tycho’s SNR and SNR 1006 are marked above the horizontal axis.

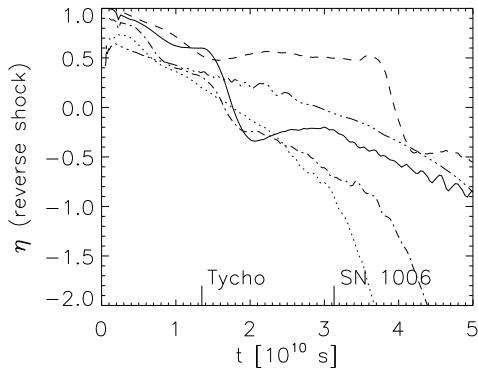


Figure 4. The same as Fig.3 but for the reverse shock.

cannot be accurately described either by a power law or

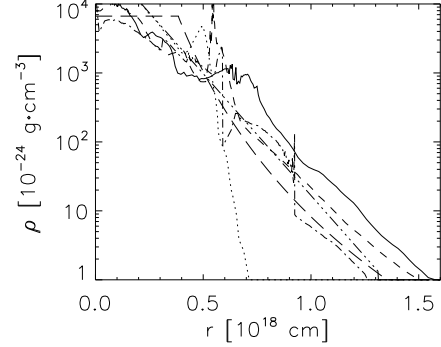


Figure 5. Comparison of the ejecta density structure from different explosion models of SNIa with the exponential ejecta profile (triple-dot-dashed line), and a power-law profile with index 7 (long-dashed line), at time 5×10^8 s after the explosion. Each of the represented SNIa models is based on a different explosion mechanism: deflagration (dotted line), delayed detonation (solid line), pulsating delayed detonation (dashed line), and sub-Chandrasekhar (dash-dotted line).

an exponential density profile for the ejecta. Instead, the simulated dynamics show a mixture of features from both these simple analytic ejecta profiles (see also Badenes & Bravo 2002).

3. DISCUSSION AND CONCLUSIONS

We have shown that the CSM structure produced by different presupernova wind models can be discriminated against an initially (at SN explosion) uniform ISM through the dynamical properties of the SNR. The expansion parameter is most sensitive to the presupernova history at SNR ages larger than that of Tycho. We have also shown that different explosion models for SNIa can be discriminated through the dynamical properties of the SNR, and through the different chemical abundances of freshly syn-

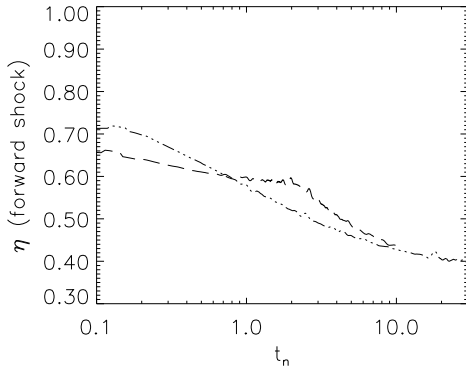


Figure 6. Expansion parameter of the forward shock as a function of time for the interaction of the analytical ejecta profiles with a constant density ISM. Due to the different ejected masses and kinetic energies of the models, the time scale has been normalized as in Dwarkadas & Chevalier (1998). The normalization timescale is 10.4×10^9 s.

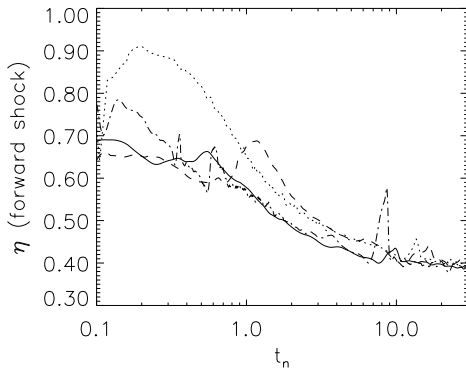


Figure 7. The same as Fig. 6 but for the numerical ejecta profiles (DEF, DDT, PDD, and SCH). Table 2 gives the corresponding normalization timescales.

thesized elements (Fe, Ca and intermediate mass elements for X-ray lines, 44Ti for γ -ray lines). The expansion parameter is most sensitive to the explosion mechanism for SNR ages shorter than that of Tycho.

The interaction of realistic CSM, produced by non-constant presupernova mass loss, with the ejecta density profiles obtained from realistic SNIa hydrodynamic calculations results in SNR configurations that show a lot of structure. Particularly interesting is the presence of several secondary shock waves traveling outwards and inwards (see Figure 8). These secondary shocks could have important consequences for the overall SNR structure and properties (magnetic field, cosmic ray acceleration, hydrodynamic instabilities, ionization structure, etc.). The denser areas in the hot, ionized intershock region will display the highest X-ray luminosity (regions outlined by the

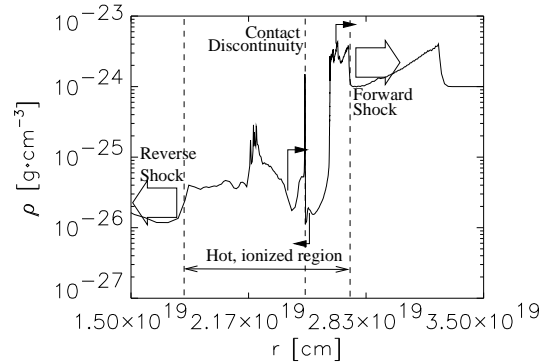


Figure 8. Detail of the structures arising as a result of the interaction of a realistic explosion model (PDD has been chosen for this example) with a CSM modified by a time-dependent wind (wind model A here). The plot shows the density profile at the age of SNR 1006, in the region between the ejecta reverse shock and the wind forward shock. The location of some secondary shocks has been marked with small arrows.

dashed vertical lines). Thermal emission is expected from these regions, dominated by lines from solar abundance plasma for the shocked CSM (density spike close to the forward shock) or by lines from the elements synthesized in the SN explosion for the shocked ejecta (density spike between the contact discontinuity and the reverse shock).

Consistent modelling of the thermal X-ray emission from SNRs remains an unsolved problem. An accurate description of nonequilibrium ionization is necessary to obtain realistic temperature and luminosity profiles (for a discussion, see e.g. Borkowski, Lyerly & Reynolds 2001). This is specially difficult for the heavy-element ejecta characteristic of SNIa. We are working on the coupling of hydrodynamical models with atomic databases to be able to produce spectra models that can be used to fit observations and thus take advantage of the high sensitivity and spectral resolution of XMM-Newton and Chandra.

ACKNOWLEDGEMENTS

This work has been supported by the MCYT grants EPS98-1348 and AYA2000-1785 and by the DGES grant PB98-1183-C03-02. C. B. is very indebted to CIRIT for a grant.

REFERENCES

- Badenes C., Bravo E., 2001, ApJ 556, L41
- Badenes C., Bravo E., 2002, in preparation
- Borkowski K., Lyerly W., Reynolds S., 2001, ApJ 548, 820
- Bravo E., Tornambé A., Domínguez I., Isern J., 1996, A&A 306, 811
- Cappellaro E. et al., 2001, ApJ 549, L215
- Dwarkadas V., Chevalier R., 1998, ApJ 497, 807
- Chevalier R., Liang E., 1989, ApJ 344, 332
- Hachisu I., Kato M., Nomoto K., 1996, ApJ 470, L97
- Immler S., Aschenbach B., Wang Q., 2001, ApJ 561, L110

- Langer N., Deutschmann A., Wellstein S., Höfflich P., 2000,
A&A 332, L9
- Schmidt B.P. et al., 1994, ApJ 434, L19
- Weaver R., McCray R., Castor J., Shapiro P., Moore R., 1977,
ApJ 218, 377